④

David Taylor Research Center

Bethesda, MD 20084–5000

Compression Testing of Thick-Section Composite Materials

by
E.T. Camponeschi, Jr.

DTIC
ELECTE
JAN 3 0 1990
S D
D CS

MAJOR DTRC TECHNICAL COMPONENTS

CODE 011 DIRECTOR OF TECHNOLOGY, PLANS AND ASSESSMENT

12 SHIP SYSTEMS INTEGRATION DEPARTMENT

14 SHIP ELECTROMAGNETIC SIGNATURES DEPARTMENT

15 SHIP HYDROMECHANICS DEPARTMENT

16 AVIATION DEPARTMENT

17 SHIP STRUCTURES AND PROTECTION DEPARTMENT

18 COMPUTATION, MATHEMATICS & LOGISTICS DEPARTMENT

19 SHIP ACOUSTICS DEPARTMENT

27 PROPULSION AND AUXILIARY SYSTEMS DEPARTMENT

28 SHIP MATERIALS ENGINEERING DEPARTMENT

DTRC ISSUES THREE TYPES OF REPORTS:

1. **DTRC reports, a formal series,** contain information of permanent technical value. They carry a consecutive numerical identification regardless of their classification or the originating department.

2. **Departmental reports, a semiformal series,** contain information of a preliminary, temporary, or proprietary nature or of limited interest or significance. They carry a departmental alphanumerical identification.

3. **Technical memoranda, an informal series,** contain technical documentation of limited use and interest. They are primarily working papers intended for internal use. They carry an identifying number which indicates their type and the numerical code of the originating department. Any distribution outside DTRC must be approved by the head of the originating department on a case-by-case basis.

Unclassified

REPORT DOCUMENTATION PAGE

1a. REPORT SECURITY CLASSIFICATION	1b. RESTRICTIVE MARKINGS
Unclassified	

2a. SECURITY CLASSIFICATION AUTHORITY	3. DISTRIBUTION / AVAILABILITY OF REPORT
	Approved for Public Release;
2b. DECLASSIFICATION / DOWNGRADING SCHEDULE	Distribution Unlimited.

4. PERFORMING ORGANIZATION REPORT NUMBER(S)	5. MONITORING ORGANIZATION REPORT NUMBER(S)
DTRC SME-89-73	

6a. NAME OF PERFORMING ORGANIZATION	6b OFFICE SYMBOL (If applicable)	7a. NAME OF MONITORING ORGANIZATION
David Taylor Research Center	Code 2802	

6c. ADDRESS (City, State, and ZIP Code)	7b. ADDRESS (City, State, and ZIP Code)
Annapolis, MD 21402	

8a. NAME OF FUNDING / SPONSORING ORGANIZATION David Taylor Research Center	8b. OFFICE SYMBOL (If applicable) Code 0113	9. PROCUREMENT INSTRUMENT IDENTIFICATION NUMBER

8c. ADDRESS (City, State, and ZIP Code)	10. SOURCE OF FUNDING NUMBERS			
	PROGRAM ELEMENT NO.	PROJECT NO.	TASK NO.	WORK UNIT ACCESSION NO
Bethesda, MD 20084	61152N			1-1720-476

11. TITLE (Include Security Classification)

(U) Compression Testing of Thick-Section Composite Materials

12. PERSONAL AUTHOR(S)

E.T. Camponeschi, Jr.

13a. TYPE OF REPORT RDT&E	13b. TIME COVERED FROM 9/87 TO 9/89	14. DATE OF REPORT (Year, Month, Day) 1989 Oct 01	15. PAGE COUNT

16. SUPPLEMENTARY NOTATION

17	COSATI CODES		18. SUBJECT TERMS (Continue on reverse if necessary and identify by block number)
FIELD	GROUP	SUB-GROUP	Composite Materials, compression, thick-section, compression failure

19. ABSTRACT (Continue on reverse if necessary and identify by block number)

Interest in the compressive response of fiber-reinforced composite materials has resulted in numerous research programs addressing the theoretical and experimental response of composites subjected to compressive loading. These research programs have dealt exclusively with the response of composite materials 6.4 mm (0.25 inches) in thickness and less. As composite materials become more attractive for use in large Navy structures, the need to understand the mechanical response of composites greater than 6.4 mm (0.25 inches) in thickness becomes a necessity.

In this program a compression test fixture that allows the testing of composites up to one inch in thickness and greater was designed and refined. This fixture was used to evaluate the effects of constituents, fiber orientation, and thickness on the compressive response of composite materials. In addition the fixture was used to determine if the failure

20. DISTRIBUTION / AVAILABILITY OF ABSTRACT	21. ABSTRACT SECURITY CLASSIFICATION
☒ UNCLASSIFIED/UNLIMITED ☐ SAME AS RPT ☐ DTIC USERS	

22a. NAME OF RESPONSIBLE INDIVIDUAL	22b. TELEPHONE (Include Area Code)	22c. OFFICE SYMBOL
E.T. Camponeschi, Jr.	(301) 267-2165	Code 2802

DD FORM 1473, 84 MAR 83 APR edition may be used until exhausted
All other editions are obsolete

mechanisms observed for thick composites are similar to those that have been observed and reported for composite materials less than 6.4 mm (0.25 in.) thick.

The strength, stiffness, and failure characteristics of 48 ply, 96 ply and 192 ply carbon/epoxy and S2 glass/epoxy are discussed. Unidirectional and (0/0/90) style laminates have been investigated. The thickness of the 96 and 192 ply coupons allows the direct measurement of NU13 for the constituents and orientations listed above and this data is also reported.

CONTENTS

FIGURES

TABLES

ABBREVIATIONS

C.V.	Coefficient of variation
DTRC	David Taylor Research Center
E_i	i-direction modulus of elasticity
ft	foot
FVF	fiber volume fraction
G_{ij}	ij-plane shear modulus of elasticity
GPa	1×10^9 Pascals
IITRI	Illinois Institute of Technology Research Institute
J	Joules
ksi	one-thousand pounds per square inch
lbs	pounds
mm	millimeter
MPa	1×10^6 Pascals
Msi	one-million pounds per square inch
NU_{ij}	ij-plane Poisson's ratio
psi	pounds per square inch
sec	second

ABSTRACT

Interest in the compressive response of fiber-reinforced composite materials has resulted in numerous research programs addressing the theoretical and experimental response of composites subjected to compressive loading. These research programs have dealt exclusively with the response of composite materials 6.4 mm (0.25 inches) in thickness and less. As composite materials become more attractive for use in large Navy structures, the need to understand the mechanical response of composites greater than 6.4 mm (0.25 inches) in thickness becomes a necessity.

In this program a compression test fixture that allows the testing of composites up to one inch in thickness and greater was designed and refined. This fixture was used to evaluate the effects of constituents, fiber orientation, and thickness on the compressive response of composite materials. In addition the fixture was used to determine if the failure mechanisms observed for thick composites are similar to those that have been observed and reported for composite materials less than 6.4 mm (0.25 in.) thick.

The strength, stiffness, and failure characteristics of 48 ply, 96 ply and 192 ply carbon/epoxy and S2 glass/epoxy are discussed. Unidirectional and (0/0/90) style laminates have been investigated. The thickness of the 96 and 192 ply coupons allows the direct measurement of NU13 for the constituents and orientations listed above and this data is also reported.

ADMINISTRATIVE INFORMATION

ASTP program, under Work Unit 1-2802-300.

INTRODUCTION

The high specific compressive strength of composite materials make them highly attractive as candidate materials for Naval applications. In many cases the material thickness required for these applications is much greater than those that have been demonstrated to date. For example, in considering composite cylinders subjected to external pressure, scale model testing has been conducted on unstiffened cylinders nominally 203 mm (8 inches) in diameter with a wall thickness of 15 mm (0.6 inches) [1].

The results from such tests have indicated that thick walled carbon reinforced composite cylinders do not reach collapse pressures expected from a 3-D stress analysis of a thick orthotropic shell [2] coupled with allowable strength from thin uniaxial compressive strength tests. A collapse pressure equating to a laminate stress of 965 MPa (140 ksi) is expected for $[0/0/90]_{ns}$ carbon/epoxy shells and wall stresses of 552-690 MPa (80 to 100 ksi) are routinely achieved. In contrast to these findings comparable tests of fiberglass reinforced cylinders [3] [4] have resulted in expected and achieved laminate strengths of 827 MPa (120 ksi).

Possible explanations for the unexpectedly low strength of thick carbon reinforced cylinders fall into the categories of

material issues, stress analysis issues, or manufacturing issues. In terms of materials issues the elastic constants or strengths determined for thin (less than 3.2 mm [0.125 inches]) materials may not be appropriate for materials that are greater than 6.4 mm (0.25 inches) in thickness. What are the trends for the compressive properties of composite materials with increasing thickness?

Stress analysis requirements that arise for thick composites include the need for fully three-dimensional analysis and the incorporation of nonlinear materials effects into these analyses should the effects be significant. The capability to perform complex 3-D stress analysis exists, yet accurate 3-D material data properties and 3-D failure criteria do not.

The manufacturing issues of concern for thick composite shells include effect of residual stress, material nonuniformity, the development of layer waviness, and the presence of material property gradients through the thickness of the component.

Certainly all of these issues are interrelated, but they could be investigated independently to identify the relative importance of each parameter with respect to the performance of thick structures. In this investigation the effect of thickness on material response and the development of 3-D compressive properties have been addressed. The elastic constants, strength and failure mechanisms of carbon and S2 glass reinforced composites are studied as a function of increasing section

thickness.

TEST METHOD DEVELOPMENT

A survey of compression test methods to identify one that would be appropriate for testing composites between 6.4 mm and 25.4 mm (0.25 and 1.00 inches) thick reveals a myriad of possible methods for materials less than 6.4 mm (.25 inches) thick, and none for greater thickness [5]. What is learned from such an investigation is that an end-loaded test coupon with simple clamping blocks on the ends was the most economical and appropriate for thick composites. The development of a fixture to test thick specimens in compression was undertaken and the following criteria were applied: the fixture must allow thick-section testing capability beginning at 6.4 mm (0.25 inches), must allow further scale up for thicker, wider, and longer specimens, must prevent load eccentricities, must allow an unsupported gage length, and must prevent splitting or brooming failures from occurring near the load introduction points.

A fixture design that met the above requirements is similar to one used by Adams [6] for 2.54 mm (0.1 inch) thick specimens, and a cross-section of the final design is shown in Fig. 1. A photograph showing the size of the 6.4 and 25.4 mm (0.25 and 1.0 inch) DTRC fixtures compared to the IITRI fixture can be found in Fig. 2. In this fixture load is applied to the ends of the specimen and clamping blocks are used to provide stability and prevent end-brooming at the point of load introduction. A

DTRC THICK-SECTION
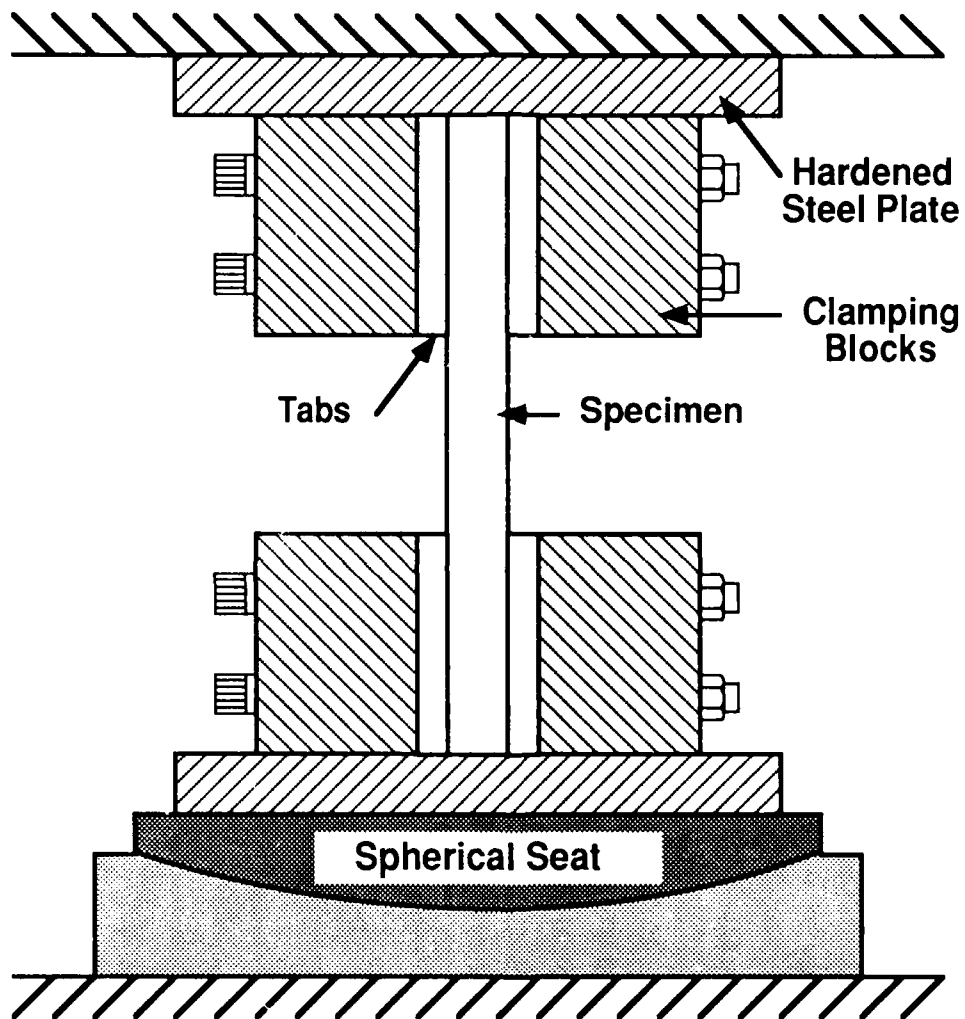# COMPRESSION TEST METHOD

Fig. 1. Schematic of DTRC thick-section compression fixture.
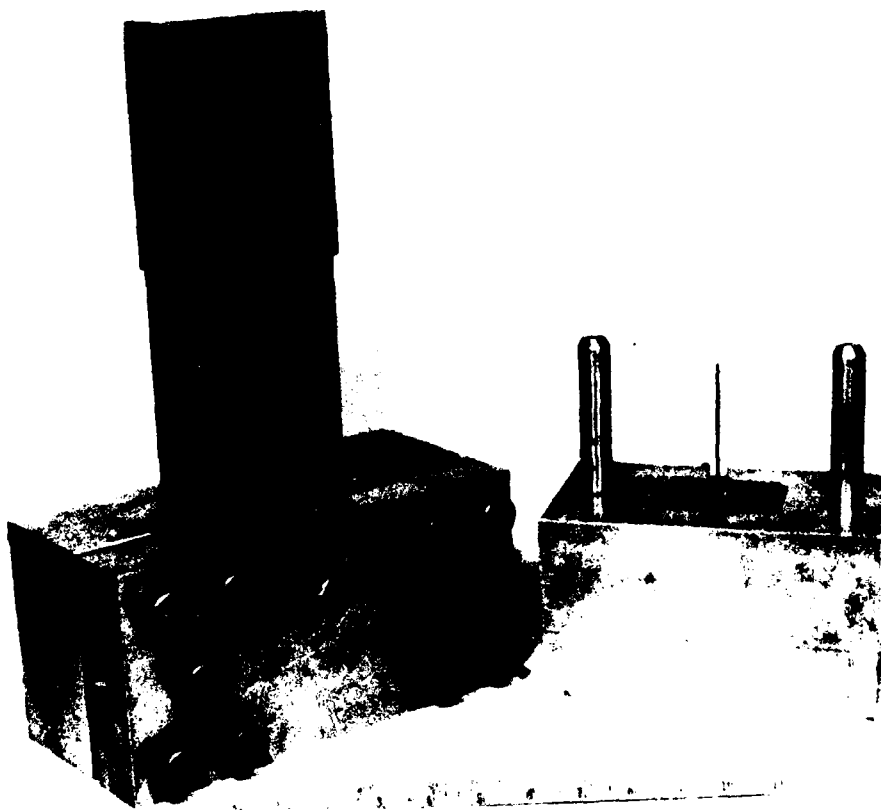
Fig. 2.   Photograph of 25.4 mm (1.0 inch) DTRC thick-section
          compression fixture and IITRI compression fixture.

6

hardened steel plate is inserted between both ends of the specimen and the test machine crosshead platens and act as load bearing surfaces. A self aligning spherical seat is placed between one end of the specimen and the load machine to assist in aligning the specimen axis and the loading axis.

Preliminary studies on test fixture design showed fixture alignment rods were unnecessary since the specimen thickness and the clamping blocks provided adequate fixture/specimen stability. These studies also showed that the size and number of clamping bolts was critical since significant bolt stresses develop due to through-thickness Poisson displacements. Initial compression tests with 48 ply specimens showed four 6.4 mm (0.25 inch) bolts in each half of the fixture could not withstand the stresses created by the specimen through-thickness Poisson effects. The following equation was developed to determine bolt stress as a function of applied longitudinal load;

$$SIG_b = \frac{(NU_{13})(SIG_c)(E_b)(E_3)(A_s)(L_c)}{(E_1)(L_b E_3 A_s + E_b A_t L_c)}$$

Where SIG_b = bolt stress
SIG_c = compression strength of composite sample
NU_{13} = through-thickness Poisson's ratio of composite sample
E_1 = longitudinal modulus of elasticity of composite material sample
E_b = modulus of elasticity of bolts
E_3 = through-thickness modulus of elasticity of composite material sample
A_t = total cross sectional area of all bolts
A_s = area of contact between sample and one

clamping block
L_b = length of bolts
L_c = thickness of composite sample

This equation provides the stress in each bolt as a function of specimen properties, specimen geometry, bolt modulus, and bolt length. The final bolt configuration consisted of 6 12.7 mm (0.5 inch) bolts for 48 ply and 96 ply specimens, and 10 15.9 mm (.625 inch) bolts for the 192 ply specimens. The bolt torque applied to each fixture prior to testing was 6.8, 20.3, 67.8 J (5, 15, and 50 ft.-lbs.) for the 48, 96 and 192 ply specimens respectively.

The crosshead displacement rate used in this investigation was chosen to provide a strain rate of approximately 0.0025 mm/mm/sec. The equivalent crosshead rates were 0.43 mm/sec. (48 ply specimen), 0.51 mm/sec. (96 ply specimen), and 1.02 mm/sec. (192 ply specimen).

MATERIAL SYSTEMS AND SPECIMEN GEOMETRY

The two material systems evaluated in this investigation were AS4/3501-6 carbon/epoxy and S2/3501-6 fiberglass/epoxy. They were chosen to investigate the effects of carbon and glass fiber reinforcements in a common epoxy matrix in light of the mechanical response observed when these fibers are used as reinforcements in thick unstiffened cylinders.

The carbon reinforced prepreg tape was supplied by Hercules Inc. and was AS4 fiber with 3501-6 350° F epoxy resin (150 g/cm^2

areal weight). The S2 glass reinforced prepreg was supplied by Fiberite and was S2 glass fiber also with 3501-6 350 F epoxy resin (205 g/cm^2 areal weight). Both systems were supplied as 12 inch wide prepreg tape and were autoclave cured at DTRC. An autoclave air temperature schedule that was slightly different than those used for thin (< 48 ply) epoxy based composites was used. This air temperature was determined from test cures on 96 and 192 ply laminates with thermocouples placed within the test panels to monitor temperature through the panel thickness during cure.

Following fabrication, samples from all panels were removed and tested for fiber volume fraction (FVF) and void content (ASTM D3171 and D2734). The following values were determined;

	48 ply	96 ply	192 ply
AS4/3501-6	58.4% /-1.33%	60.0% / 0.34%	60.3% /-0.57%
S2/3501-6	57.6% / 0.27%	53.8% / 0.97%	58.0% / 0.64%

Three panel thicknesses were fabricated for this investigation; 48 ply, 96 ply, and 192 ply. Specimens were machined from these panels resulting in nominal specimen thicknesses of 6.4, 12.7, and 25.4 mm (0.25, 0.50 and 1.0 inches). [0] and [0/0/90]$_{ns}$ laminate stacking sequences were fabricated for the 48 and 96 ply panels, and [0/0/90]$_{ns}$ were fabricated for the 192 ply panels. The specimens were designed so that the width was 4 times the specimen thickness, the gage length was 5 times the specimen thickness, and the tab length was

5 times the specimen thickness (with a minimum tab length of [2.5 inches]). The nominal specimen dimensions are summarized in Table 1 and the specimen geometry is shown is Fig. 3.

Table 1. Nominal specimen dimensions

	48 Ply	96 Ply	192 Ply
Thickness mm (inches)	6.4 (0.25)	12.7 (0.50)	25.4 (1.0)
Width mm (inches)	25.4 (1.0)	50.8 (2.0)	101.6 (4.0)
Length mm (inches)	158.8 (6.25)	190.5 (7.5) & 165.1 (6.5)	381.0 (15.0)
Gage Length mm (inches)	31.8 (1.25)	63.5 (2.5) & 38.1 (1.5)	127.0 (5.0)
Tab Length mm (inches)	63.5 (2.5)	63.5 (2.5)	127.0 (5.0)
Tab Thickness mm (inches)	3.2 (0.125)	3.2 (0.125)	4.4 (0.25)

The maximum allowable specimen gage section length was determined on the basis of a Euler column buckling analysis that assumed the specimen acts a as pinned end column and that includes the effects of transverse shear [7]. The expression for the allowable length/thickness ratio is:

$$\frac{l}{t} = 0.9069 \left[\frac{E_x}{Y_{ult}} \left(1 - 1.2 \frac{Y_{ult}}{G_{xz}} \right) \right]^{\frac{1}{2}}$$

where
l = specimen length $\qquad$ E_x = longitudinal modulus

t = specimen thickness $\qquad$ G_{xz} = through-thickness shear modulus

10

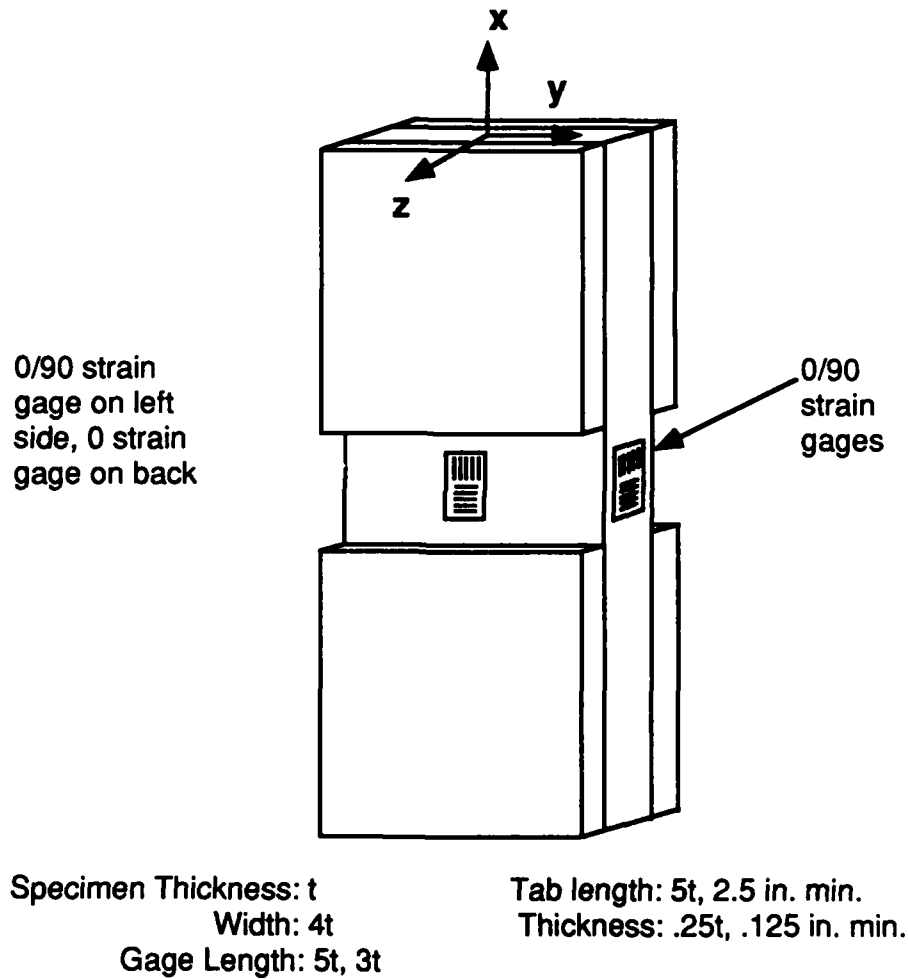# SPECIMEN GEOMETRY

Fig. 3. Specimen geometry, material directions, and strain gage locations.

Y_{ult} = ultimate compressive
          strength

For the materials and orientations used in this study the maximum
allowable gage lengths are:

[0] S2/glass/epoxy -- 5.1

[0/0/90] S2/glass/epoxy -- 5.3

[0] AS4/epoxy -- 6.5

[0/0/90] AS4/epoxy -- 7.8

Five specimens of each thickness and orientation were
evaluated for the 48 and 192 ply thicknesses, and four of each
(two with a 3:1 l/t ratio and two with a 5:1 l/t ratio) were
evaluated for the 96 ply thickness. Foil backed electrical
resistance strain gages were used in this investigation to
monitor strain. Single gages or unstacked 0/90 CEA-06 type gages
were used with lengths of 3.2 or 6.4 mm (.125 of .250 inches)
The 48 ply and one-half of the 96 ply specimens were instrumented
with a longitudinal gage on each face. The remaining half of the
96 ply and all of the 192 ply specimens were instrumented with
strain gages on both faces and both edges as shown in Fig. 3.

RESULTS AND DISCUSSION

The results from this program include longitudinal modulus
of elasticity, inplane and through-thickness Poisson's ratio,
ultimate compression strength, and ultimate compression strain at
failure. These data as well as the observed failure mechanisms

12

are discussed in the next three sections. Tables 2 and 3 summarize the elastic constant, strength, and strain-to-failure data.

ELASTIC CONSTANTS

The longitudinal modulus of elasticity (E_x) was recorded for all three specimen thicknesses and NU_{xy} and NU_{xz} were recorded for the 96 ply and 192 ply specimens. The E_x data from Table 3 is represented in graphical form in Fig. 4. This plot shows that the longitudinal moduli for these materials is independent of specimen thickness. The values of E_x can be adjusted for fiber volume fraction effects from 115.8 GPa (16.8 Msi) (60 % FVF) for the [0] AS4/3501-6 converts to 125.5 GPa (18.2 Msi) (65 % FVF) and from 51.0 GPa (7.4 Msi) (55 % FVF) to 60.0 GPa (8.7 Msi) (65 % FVF) for the [0] S2/3501-6 specimens.

A comparison of NU_{xy} and NU_{xz} for the unidirectional 92 ply specimens show both the carbon and fiberglass materials to be transversely isotropic. The measured values of NU_{xz} for the $[0/0/90]_{ns}$ laminates was compared to theoretically predicted value in reference [8] and agree well.

When reducing the strain-strain data used to determine NUxz for the $[0/0/90]_{ns}$ laminates, significant nonlinearities in the curves were observed as shown in Fig. 5. These nonlinearities were quantified by comparing the initial and final slope of the NU_{xz} strain-strain curves. The initial slope was determined by the secant tangent method between .1 and .3 percent strain, and

13

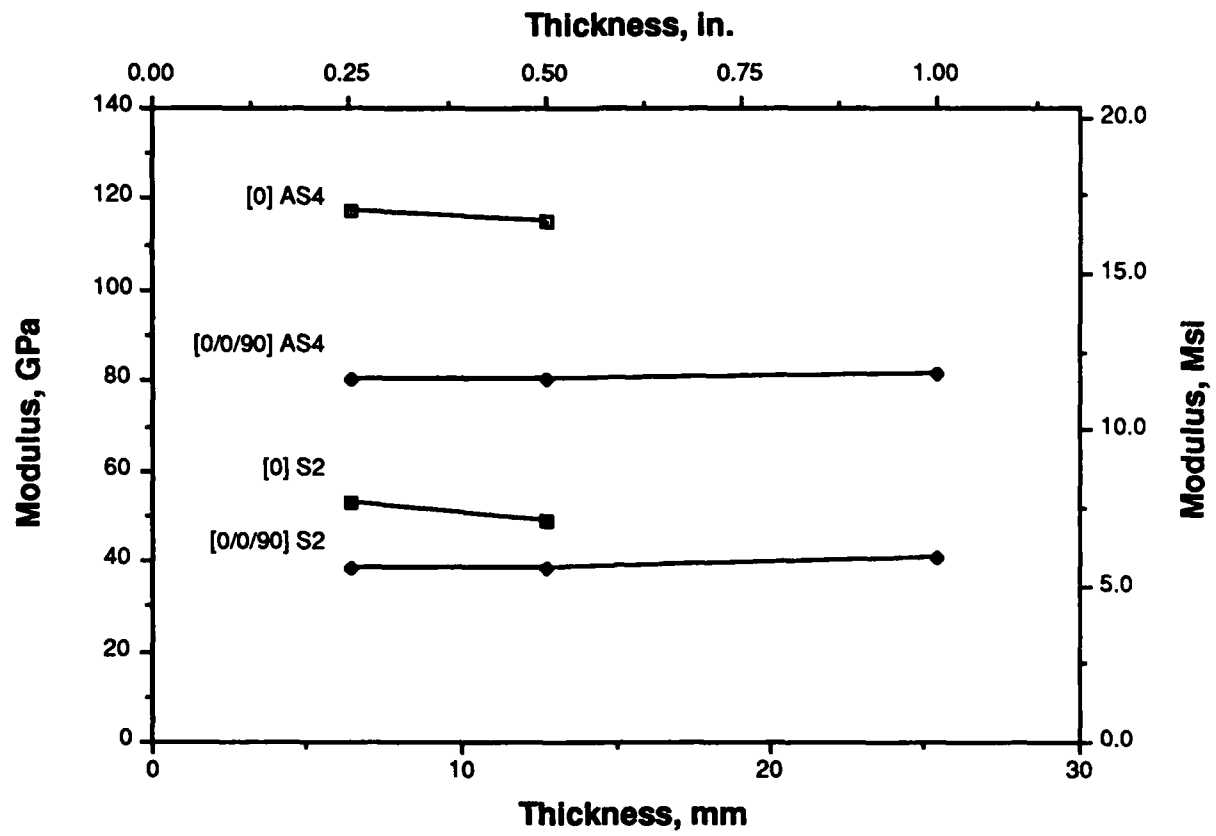**Longitudinal Modulus as a Function of Thickness**

Fig. 4. Longitudinal modulus as a function of thickness.
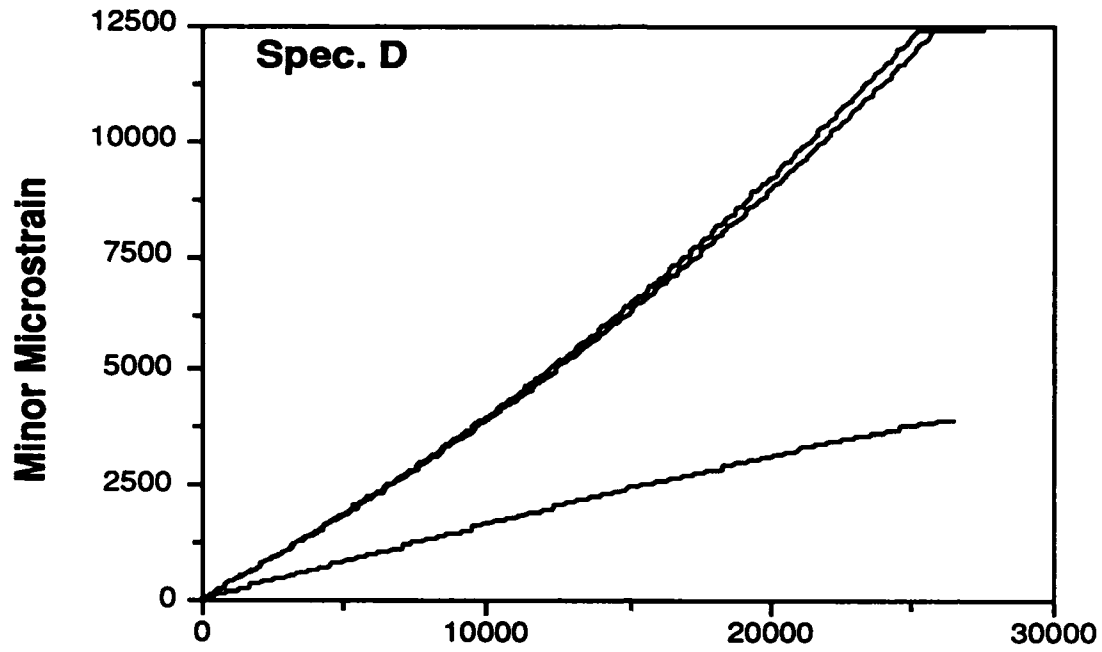
96 Ply [0/0/90] S2/Epoxy

Fig. 5. Through-thickness Poisson's ratio nonlinearity.

Table 2. Summary of Elastic Constant Results

Longitudinal Modulus, GPa (Msi)

	AS4/3501-6		S2/3501-6	
No. Plies	[0]	[0/0/90]	[0]	[0/0/90]
48	117.1 (16.99)	80.26 (11.64)	52.86 (7.66)	41.37 (6.00)
96	115.0 (16.68)	79.98 (11.60)	49.02 (7.11)	38.27 (5.55)
192	--	81.22 (11.78)	--	40.75 (5.91)

NU_{xy}

	AS4/3501-6		S2/3501-6	
No. Plies	[0]	[0/0/90]	[0]	[0/0/90]
48	--	--	--	--
96	.332	.067	.290	.157
192	--	.068	--	.167

NU_{xz}

	AS4/3501-6		S2/3501-6	
No. Plies	[0]	[0/0/90]	[0]	[0/0/90]
48	--	--	--	--
96	.322	.450	.306	.363
192	--	.472	--	.357

Table 3. Summary of strength and strain-to-failure results

Ultimate Compression Strength, MPa (ksi)

No. Plies	AS4/3501-6		S2/3501-6	
	[0]	[0/0/90]	[0]	[0/0/90]
48	1160 (168.2)	1067 (154.7)	1275 (184.9)	988.7 (143.4)
96	852.2 (123.6)	891.5 (129.3)	976.3 (141.6)	930.1 (134.9)
192	--	841.9 (122.1)	--	797.8 (115.7)

Longitudinal Strain-to-Failure, %

No. Plies	AS4/3501-6		S2/3501-6	
	[0]	[0/0/90]	[0]	[0/0/90]
48	1.00	>1.48	2.56	2.46
96	.79	1.26	2.06	2.62
192	--	1.16	--	2.01

the final slope was determined by the same method between strain-at-failure and .2 percent less than strain-at-failure. The results of this comparison are shown in Fig. 6. Since the nonlinearities in NU_{xz} were so significant a test was conducted on two 192 ply laminates to determine if the nonlinearities were reversible. For one AS4 and one S2 glass reinforced coupon the first compression test was conducted to 75 % of ultimate stress, the load was slowly reversed and the specimen was reloaded to
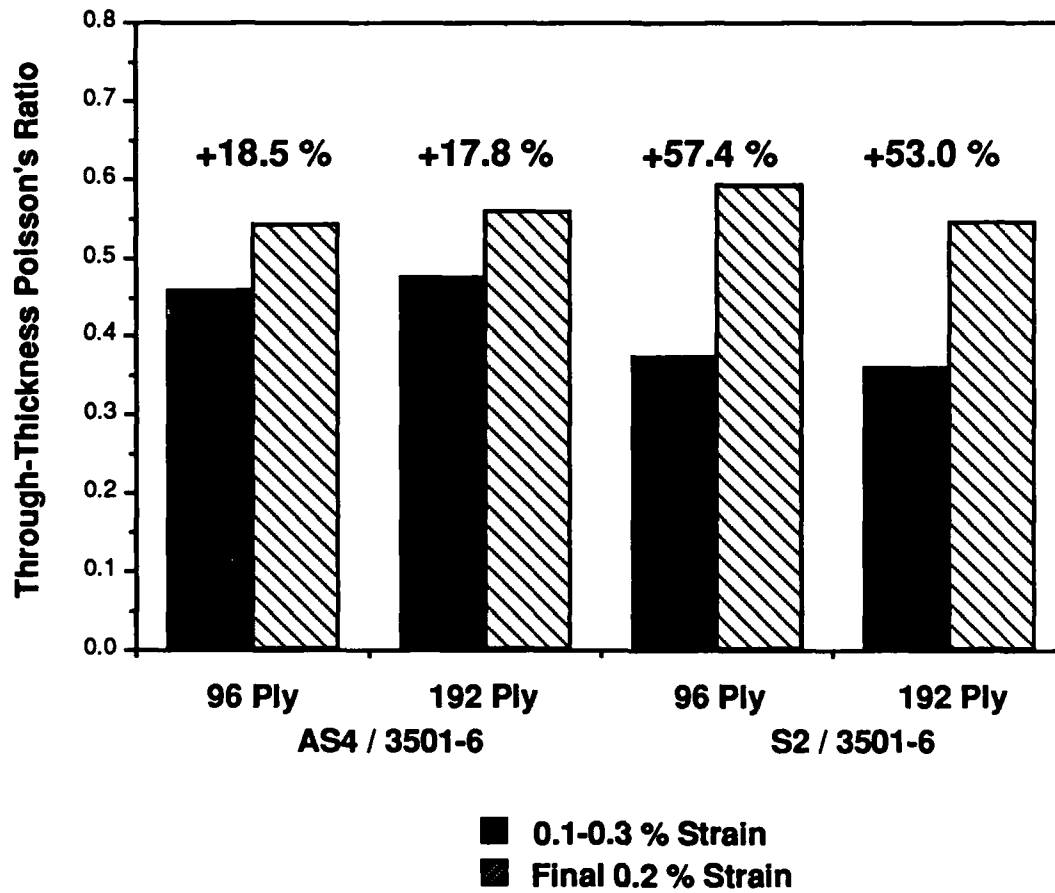
NUxz Change for [0/0/90] Laminates

Fig. 6.   NUxz change for [0/0/90]$_{ns}$ laminates.

failure. The strain-strain data for the test to failure tracked the data for the initial test, attributing this nonlinearity to a reversible phenomena and not damage development.

The strain gages used to determine NU_{xz} were mounted on the edge of the compression test specimens as described earlier, so the effect of free-edge stresses must be considered when analyzing the edge strain data. To estimate the sign and magnitude of the sigma z stress a free-edge stress analysis that utilizes a force and moment balance in the free-edge zone as suggested by Pagano and Pipes [9] was performed. This analysis indicated that the sigma z stresses on the free-edge of the 192 ply carbon and S2 glass laminates is less than 13.8 MPa (2 ksi) and is compressive. Therefore the effect of these stresses would be to decrease the free-edge Poisson strains compared to strains away from the free-edges, making the edge-measured NU_{xz} nonlinearities more conservative than in the center of the laminates.

A similar comparison for nonlinearities seen in the longitudinal moduli is shown in Fig. 7. These nonlinearities are not as significant as those for NU_{xz} however a drop in modulus of 20 % could significantly effect strength and stability analyses for thick composite shells.

Nonlinearities for the longitudinal modulus and NU_{13} for the unidirectional specimens were also measured and the results are summarized below;
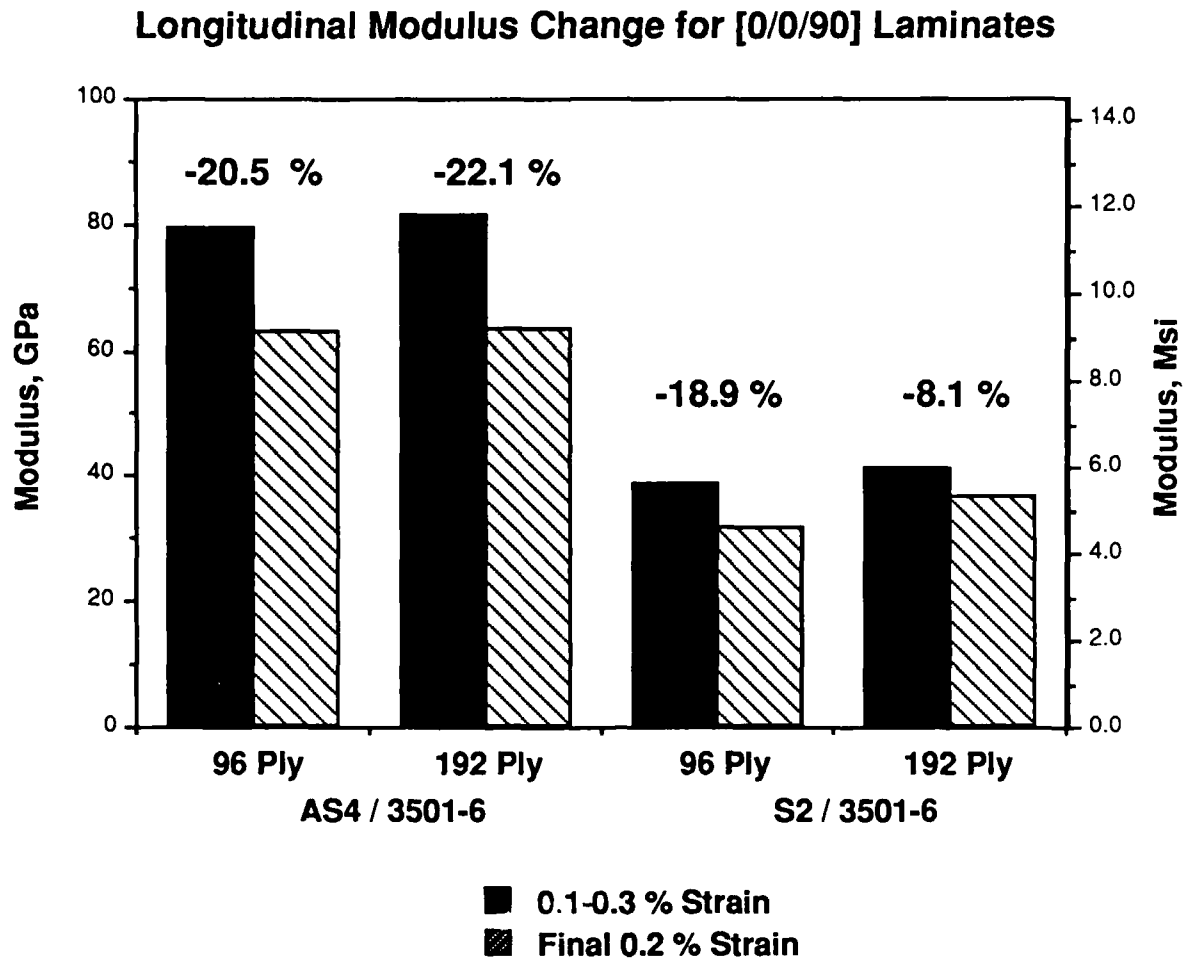
19

Longitudinal Modulus Change for [0/0/90] Laminates

Fig. 7. Longitudinal modulus change for $[0/0/90]_{ns}$ laminates.

	AS4/3501-6	S2 glass/3501-6
Ex	10 % decrease	no change
NU13	12.1 % increase	12.9 % increase

ULTIMATE COMPRESSION STRENGTH

Figure 8 shows the ultimate compressive strength as a function of specimen thickness for both materials and orientations. These curves show a sharp decrease in compression strength with increasing thickness for the unidirectional specimens. Even at a thickness of 6.4 mm (0.25 in.) the strength of the unidirectional carbon and fiberglass coupons was lower than strengths determined using shear loading test techniques such as the IITRI, Celanese, or sandwich beam methods documented in ASTM D3410 . Unidirectional compression strengths from end-loaded coupons are typically reported to be lower than from the methods in D3410 [10] [11], and the strengths measured using 6.4 mm (0.25 inch) thick specimens in this investigation are comparable to those previously reported. Due to the continually decreasing strength in testing 12.7 mm thick unidirectional specimens and the lack of interest in nesting large numbers of unidirectional plies even in thick laminates, no 192 ply unidirectional coupons were fabricated or tested.

The strength of the AS4/epoxy $[0/0/90]_{ns}$ laminates dropped 13.8 % in going from 6.4 to 12.7 mm (0.25 to 0.5 inches) and dropped 5.6 % in going from 12.7 to 25.4 mm (0.5 to 1.0 inches).
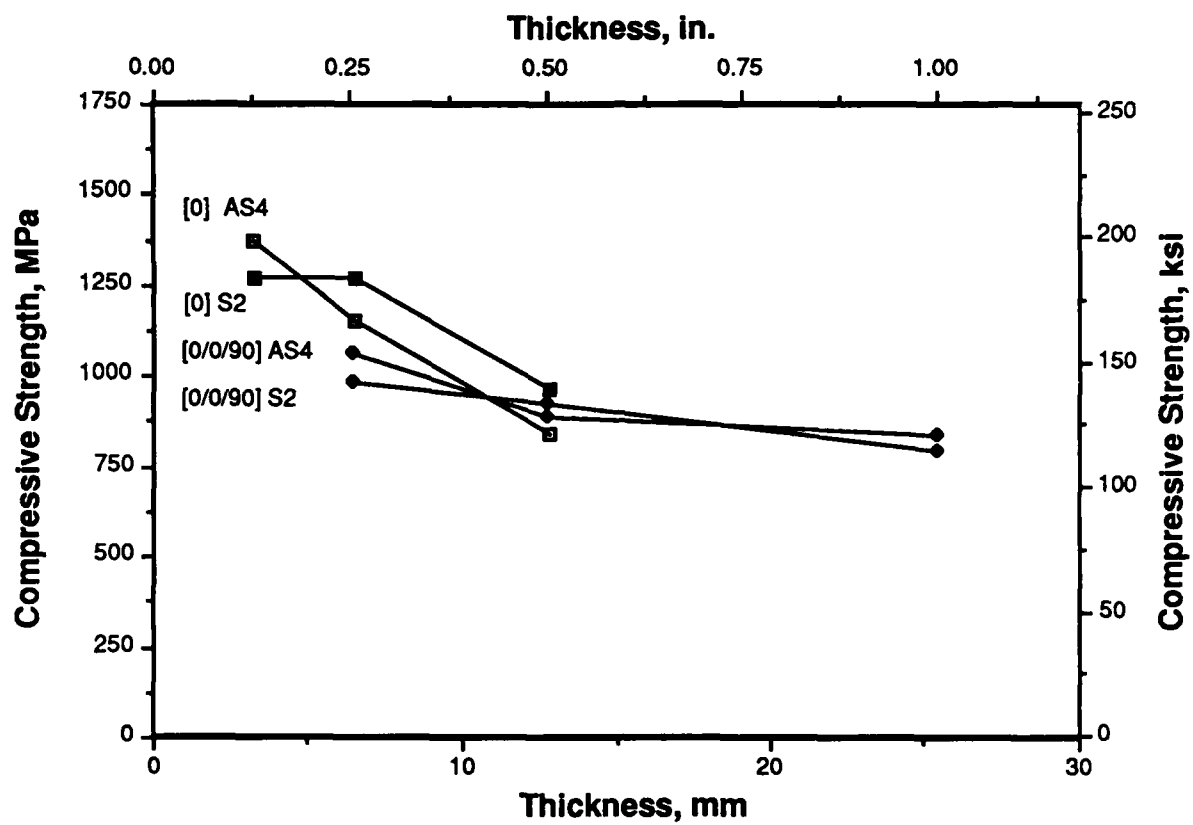
Strength as a Function of Thickness

Fig. 8. Strength as a function of thickness.

The S2 glass/epoxy laminates showed a lower decrease from 6.4 to 12.7 mm (0.25 to 0.5 inches) (9.9 %) than from 12.7 to 25.4 mm (0.5 to 1.0 inches) (14.2 %). Although this trend of decreasing strength with increasing thickness appears significant it should be considering that the volume of these specimens is increasing much more quickly than the thickness. The $[0/0/90]_{ns}$ specimens reported above drop roughly 20 % when increasing the thickness from 6.4 to 25.4 mm (0.25 to 1.0 inches), or by a factor of four. By contrast the same drop in strength occurs with a specimen volume increase from 25.56 cm^3 (1.56 in.^{3}) to 1229 cm^3 (75 in.^{3}), or by a factor of 48. Considering that it is widely believed that compression failure in composite materials is triggered by local events then this trend in strength is encouraging for the order of magnitude increase in material volume. In fact it is believed that further reductions in strength would not be seen with significantly thicker specimens.

One other fact determined in the strength study is that the low compressive strength experienced in thick, unstiffened, carbon reinforced composite cylinders is not attributable to the effect of thickness on uniaxial compressive strength. That is the strength of the thick $[0/0/90]_{ns}$ AS4/epoxy coupons did not drop to a level of 552-690 MPa (80-100 ksi) as seen in testing of thick-walled shells.

FAILURE MECHANISMS

The failure mechanisms observed in fractured specimens were

similar for all of the specimen thicknesses tested. Failures consistently occurred at either the gage-section tab intersection point or the specimen ends. Failures at the specimen ends were well restrained by the clamping blocks and the resulting failure characteristics were well maintained. In contrast failure that occurred at the gage-section tab intersection resulted in excessive delamination since there was no through-thickness restraint. Figures 9 and 10 show the 96 and 192 ply $[0/0/90]_{ns}$ fractured specimens.

The dominant characteristics at both failure locations were shear planes and kink bands. The kink bands were located along the shear planes and varied in dimension. The shear planes for all specimens except the unidirectional carbon/epoxy were oriented through the thickness, that is straight across the width of the specimen and at an angle through the thickness. The shear plane of the unidirectional carbon/epoxy specimens was oriented at an angle across the coupon width, and straight through the thickness. Figure 11 shows a close-up of the kink-bands on the ends of a carbon and S2 glass 96 ply laminate. Figure 12 shows kink-bands at the gage-section tab intersection for two 192 ply specimens.

The predominant difference in the failure characteristics between the carbon and S2 glass 25.4 mm (1.0 inch) thick coupons is that the carbon coupons completely separated upon failure whereas the S2 glass coupons remained intact.

24

$[0/0/90]_{16S}$
AS4/3501-6

$[0/0/90]_{16S}$
S2/3501-6

Fig. 9.   96 ply $[0/0/90]_{16s}$ fractured specimens.

25

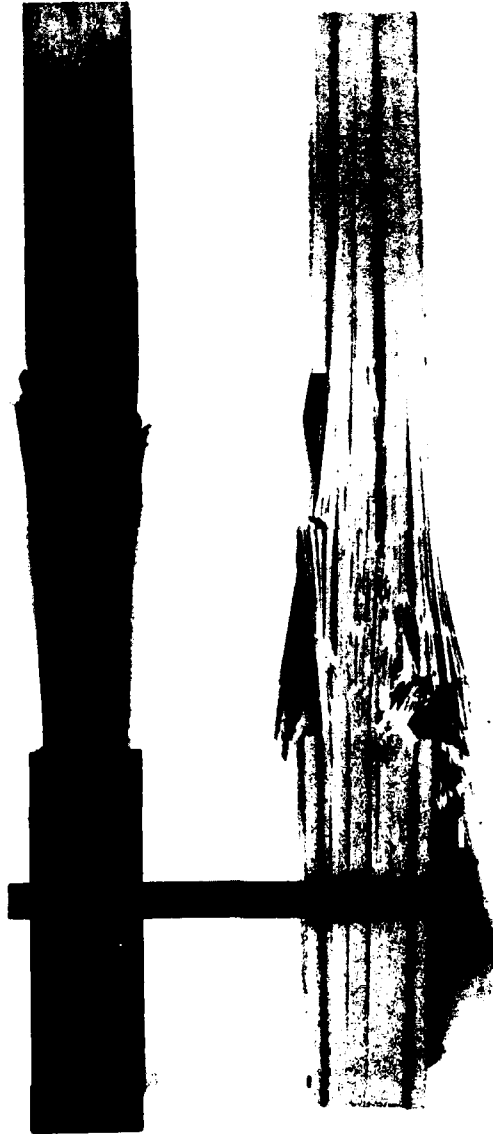**[0/0/90]₃₂s**   **[0/0/90]₃₂s**

AS4/3501-6   **S2/3501-6**

Fig. 10. 192 ply [0/0/90]₃₂s fractured specimens.

$[0/0/90]_{16S}$
AS4/3501-6

$[0/0/90]_{16S}$
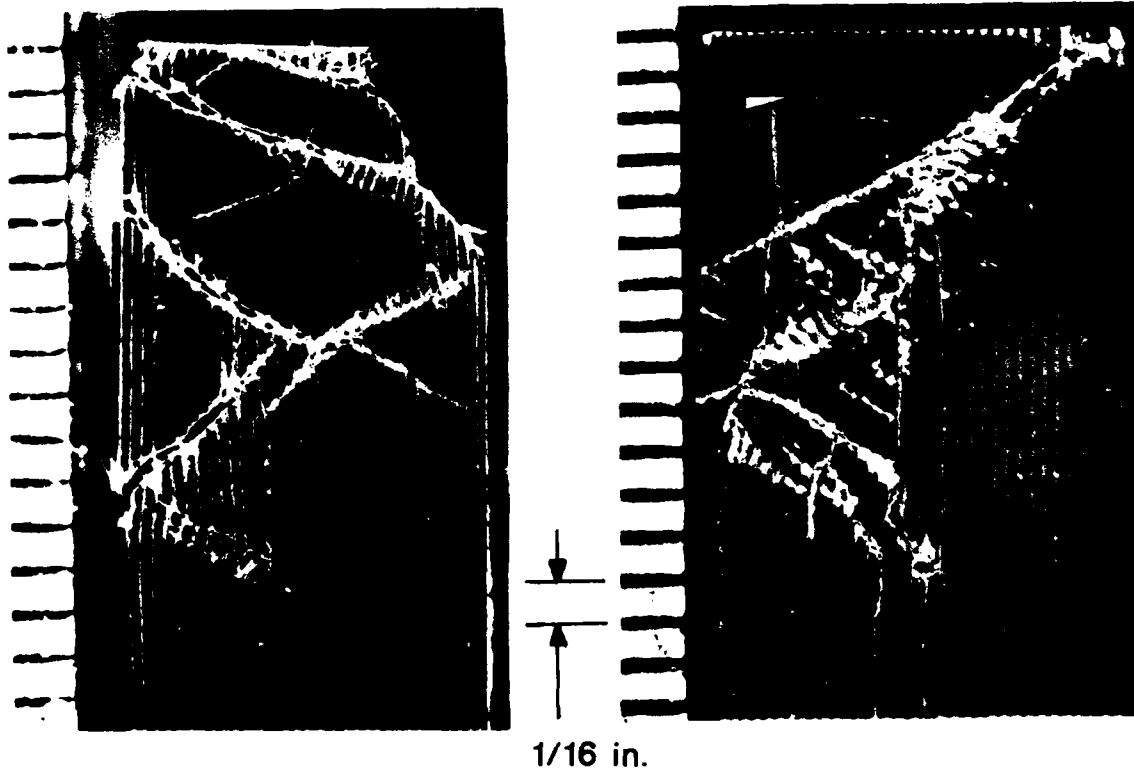S2/3501-6

1/16 in.

Fig. 11. Close-up of kink-bands in 96 ply $[0/0/90]_{16S}$ specimens.

[0/0/90]$_{32S}$
AS4/3501-6　　　**[0/0/90]**$_{32S}$
S2/3501-6

Fig. 12.　Close-up of kink-bands in 192 ply [0/0/90]$_{32s}$
specimens.

CONCLUSIONS

The conclusions from this investigation concern the effect of thickness on the compressive response of [0] and $[0/0/90]_S$ carbon and fiberglass reinforced composite materials. The longitudinal modulus of these materials was insensitive to sample thickness. The inplane and through-thickness Poisson's ratios were also independent of thickness, however large changes in the through-thickness Poisson's ratio with applied load were observed for the $[0/0/90]_S$ laminates. A change in NU_{xz} of 57.4 % was recorded for the S2/3501-6 laminates.

The strength of the [0] specimens was very sensitive to thickness in tests conducted on coupons up to 12.7 mm (0.5 in.) thick. The $[0/0/90]_S$ laminates showed a decrease in strength of approximately 22 % from 6.4 mm (0.25 in.) to 25.4 mm (1.0 in.). The failure characteristics for both materials in all thicknesses was similar to observations regularly reported for thin composite coupons. The presence of shear planes and kink-bands through the specimen thickness predominated. Delaminations were routinely observed propagating from the kink-bands and resulted in excessive damage development when failures occurred in the vicinity of the gage-section. When failures occurred within the clamping blocks delamination was suppressed and the resulting failure characteristics were much more preserved.

In reference to the objective of this research as summarized in the introduction, the trends in material properties, strength

and failure mechanisms of thick composites do not account for the observed response of thick composite shells when subjected to hydrostatic pressure. The strength of thick, carbon reinforced laminates has been found to be at least as high as for thick fiberglass reinforced laminates. With the exception of the nonlinearities seen in the through-thickness Poisson's ratio, the material elastic constants reported are equivalent to those found in thin coupons. The effect of the these nonlinearities on shell response will not be known until these effects are incorporated in 3-D shell analysis. However since the nonlinearties reported are greater for the fiberglass than the carbon composites, it appears that they will not provide an explanation for the poor response of thick unstiffened carbon reinforced shells compared to fiberglass shells

REFERENCES

1. Garala, H. J., "Experimental Evaluation of Graphite/Epoxy Composite Cylinders Subjected to External Hydrostatic Compressive Loading," Proceedings of the 1987 Spring Conference on Experimental Mechanics, Society for Experimental Mechanics, pp. 948-951 (1987).

2. Lekhnitskii, S. G., Theory of Elasticity of an Anisotropic Body, Mir Publishers, Moscow, (1981).

3. Dally, J. W., Nelson, H. R., and Cornish, R. H., "Fatigue and Creep Properties of Glass-Reinforced Plastic Under Compressive States of Stress," ASME Paper No. 63-WA-236, Dec. (1963).

4. Hom, K., Buhl, J. E., and Couch, W. P., "Hydrostatic Pressure Tests of Unstiffened and Ring-Stiffened Cylindrical Shells Fabricated of Glass-Filament Reinforced Plastics," David Taylor Model Basin Report 1745, Sept. (1963).

5. Camponeschi, E. T., Jr. "Compression of Composite Materials: A Review," David Taylor Research Center Report, DTRC-87-050, November (1987).

6. Irion, M. N. and Adams, D. F., "Compression Creep Testing of Unidirectional Composite Materials," Composites, 12 #2:117-123 (1981).

7. Timoshenko, S. P. and Gere J. M., Theory of Elastic Stability, McGraw-Hill, New York (1961).

8. Camponeschi, E. T., Jr., "Through-Thickness Strain Response of Thick Composites in Compression," David Taylor Research Center Report DTRC SME-89-67 (1989).

9. Pagano, N. J. and Pipes, R. B, "Influence of Stacking Sequence on Laminate Strength," Journal of Composite Materials, 5 #1:50-57 (1971).

10. Shuart, M. J., "Failure of Compression-Loaded Multi-Directional Composite Laminates," AIAA/ASME/ASCE/AHS 29th Structures, Structural Dynamics and Materials Conference, AIAA Paper No. 88-2293 (1988).

11. Berg, J. S. and Adams, D. F., "An Evaluation of Composite Material Compression Test Methods," Univ. of Wyoming Report UW-CMRG-R-88-106 (1988).

INITIAL DISTRIBUTION

Copies				CENTER DISTRIBUTION		
				Copies	Code	Name
12	DTIC					
3	NAVSEA			1	0115	Caplan
	1	05M3	(Pinto)			
	1	92R	(Swan)	1	0113	Douglas
3	NRL			1	17	Krenzke
	1	6383	(Badaliance)			
	1	6383	(Wolock)	1	172	Rockwell
	1	6385	(Chaskelis)			
				1	176	Sykes
1	NSWC					
	1	R31	(Augl)	1	1720.2	Phyillaier
1	ONT			1	1720.4	Wiggs
	1	225	(Kelly)			
				1	1730.2	Critchfield
1						

1
Dr. Don Adams
ME Dept.
Univ. of Wyoming
Laramie, WY 82071

1
Ken Cheverton
SPARTA Inc.
4520 Executive Dr., Suite 210
Chicago, IL 60616

1
Dr. Reaz Chaudhuri
Dept. of Civil Eng.
3220 Merrill Eng. Bldg.
Univ. of Utah
Salt Lake City, UT 84112

1
Dr. H. T. Hahn
The Pennsylvania State Univ.
227 Hammond Building
University Park, PA 16802

Copies	Code	Name
1	2723	Wilhelmi
1	274	Wang
1	28	Wacker
1	2801	Crisci
1	2802	Morton
25	2802	Camponeschi
1	2803	Cavallaro
1	284	Fischer
1	2844	Castelli
1	522.2	TIC (A)
1	522.1	TIC (C)
1	5231	Office Services

1
K. E. Hofer
L. J. Broutman & Assoc. Ltd.
3424 South State St.
Chicago, IL 60616

1
Subhash Khatri
Materials Eng. Dept.
Drexel Univ.
Philadelphia, PA 19104

1
Dr. R Sierakowski
Chairman, Civil Eng. Dept.
Ohio State Univ.
2070 Neil Ave.
470 Hitchcock Hall
Columbus, OH 43210

1
K. A. Stubenhofer
Information Center
Lord Corp.
PO Box 10039
Erie, PA 16514

1
Dr. Steve Yurgartis
ME Dept.
Clarkson Univ.
Potsdam, NY 13676

1
Dr. J. R. Vinson
Dept. of Mech. Engineering
Spencer Laboratory
Univ. of Delaware
Newark, DE 19716

1
Dr. R. K. Eby
Materials Science and Engineering
102 Maryland Hall
The Johns Hopkins University
Baltimore, MD 21218

1
Dr. D. Wilkins
Director, CCM
University of Delaware
Newark, DE 19716

1
Ms. E. Gail Guynn
1201 Harvey Road, #24
College Station, TX 77843

1
Mr. Jack Woods
Foster Miller
350 Second Avenue
Waltham, MA 02154

1
Mr. Ray Garvey
Oak Ridge National Laboratory
P.O. Box 2003
Oak Ridge, TN 37831-7294

1
Mr. Mark Sherman
Amoco Research Center
P.O. Box 400
Naperville, Il 60566

1
Dr. Mark Shuart
Langley Research Center
Mail Code 190
Hampton, VA 23665

1
Dr. Bruce Trethewey
BASF Structural Materials Inc.
TPC
13504-A Southpoint Boulevard
Charlotte, NC 28217

1
Dr. R.B. Pipes
Dean of Engineering
University of Delaware
Newark, DE 19716

1
Anough Poursartip
Dept. of Metals & Materials Engineering
University of British Columbia
309-6350 Stores Road
Vancouver, British Columbia
Canada V6T 1W5

1
John M. Winter, Jr.
Center for Nondestructive Evaluation
102 Maryland Hall
The Johns Hopkins University
Baltimore, MD   21218

1
Mohamed G. Abdallah, Ph.D., P.E.
Hercules Incorporated
Science and Technology Department
Bacchus Works
Magna, UT   84044-0098

1
Thomas K. Tsotsis, Ph.D.
Composite Materials
CIBA-GEIGY Corporation
5115 East La Palma Avenue
Anaheim, CA   92807-2018

1
John H. Bode, Ph.D., P.E.
Honeywell Inc.
Armament Systems Division
MN48-2500
7225 Northland Drive
Brooklyn Park, MN   55428

1
Don E. Pettit
Composites Development Center
Lockheed
Aeronautical Systems Company
D74-72, B369, B6
Burbank, CA   91520-7004

1
K. Benjamin Su
E. I. Du Pont De Nemours & Company
Engineering Technology Laboratory
Experimental Station - 80304
Wilmington, DE   19880-0304

1
T.H. Tsiang, Sc.D.
Lockheed
Aeronautical Systems Company
Burbank, CA   91520-4717

1
R. H. Boschan
Composites Development Center
Lockheed
Aeronautical Systems Company
Burbank, CA   91520-7637

1
Anthony A. Caiazzo, P.E.
Materials Science Corporation
Gwynedd Plaza II
Spring House, PA   19477

1
Douglas S. Cairns, Ph.D.
Hercules Incorporated
Science & Technology Department
Bacchus Works
Magna, UT   84044-0098

1
Dr. David Cohen
Hercules Aerospace Company
Missiles, Ordnance & Space Group
Bacchus Works
Magna, UT   84044-0098

1
Ori Ishai, D.Sc.
Professor, Faculty of Mechanical
 Engineering
Technion - Israel Institute of
 Technology
Technion, Haifa 32000, Israel

1
John Morton, D. Phil
Engineering Science & Mechanics
 Department
Virginia Polytechnic Institute
 and State University
Blacksburg, VA   24061

1
Vasilios Peros
Martin Marietta
Aero & Naval Systems
103 Chesapeake Park Plaza
Baltimore, MD 21220

1
John W. Gillespie, Jr., Ph.D.
Center for Composite Materials
Composites Manufacturing Science Laboratory
University of Delaware
Newark, DE 19716

1
Dr. Donald L. Hunston
Polymer Composites Group
Polymers Division
National Institute of Standards
 and Technology
Building 224, Room A209
Gaithersburg, MD 20899

1
Prof. A. J. Vizzini
The University of Maryland
College of Engineering
Department of Aerospace Engineering
College Park, MD 20742

1
Dr. Fuh-Gwo Yuan
Department of Mechanical
 & Aerospace Engineering
North Carolina State University
Raleigh, NC 27695-7910